European Journal of Drug Metabolism and Pharmacokinetics (2020) 45:801–808
https://doi.org/10.1007/s13318-020-00639-z

SHORT COMMUNICATION

The Influence of Paracetamol on the Penetration of Sorafenib and Sorafenib N-Oxide Through the Blood–Brain Barrier in Rats

Agnieszka Karbownik[1] · Joanna Stanisławiak-Rudowicz[2] · Anna Stachowiak[1] · Michał Romański[3] · Edmund Grześkowiak[1] · Edyta Szałek[1]

Published online: 10 August 2020

Abstract

Background and Objective Sorafenib is an oral, multikinase inhibitor with established single-agent activity in several tumor types. Sorafenib was moderately transported by P-glycoprotein (P-gp) and more efficiently by breast cancer resistance protein. The constitutive androstane receptor (CAR) is a ligand-activated transcription factor involved in P-gp regulation in the brain microvasculature. Paracetamol is a CAR activator. The purpose of this study was to investigate the effect of paracetamol on the brain uptake of sorafenib and sorafenib N-oxide.

Methods The rats were assigned to two groups—rats receiving oral paracetamol 100 mg/kg and sorafenib 100 mg/kg ($n=42$, I_{SR+PA}) and rats receiving oral vehicle and sorafenib 100 mg/kg ($n=42$, II_{SR}). The sorafenib and sorafenib N-oxide concentrations in blood plasma and brain tissue were determined by a high-performance liquid chromatography method with ultraviolet detection. Brain-to-plasma partition coefficient (K_p) was calculated as a ratio of the area under the curve from zero to 24 h (AUC) in the brain and plasma. A drug targeting index (DTI) was estimated as the group I_{SR+PA} K_p to group II_{SR} K_p ratio.

Results Pharmacokinetic analysis revealed increased brain exposure to sorafenib and sorafenib N-oxide after co-administration of paracetamol. The brain maximum concentration (C_{max}) and the AUC of the parent drug in the I_{SR+PA} group compared with the II_{SR} group were greater by 49.5 and 77.8%, respectively, and the same parameters for the metabolite were higher by 51.4 and 50.9%. However, the K_p values of sorafenib and sorafenib N-oxide did not differ significantly between the two animal groups and the DTI values were close to 1.

Conclusion Paracetamol increases exposure to sorafenib and sorafenib N-oxide in the brain, likely due to increased exposure in plasma.

1 Introduction

According to the World Health Organisation (WHO), the number of cancer cases is increasing despite better access to healthcare in the 21st century. Cancers are some of the major causes of deaths worldwide [1]. Hepatocellular carcinoma (HCC) is the sixth most common cancer in the world and the fourth most common cause of cancer mortality. Survival ranges from 6 to 9 months depending on the stage of the disease at the time of diagnosis and the treatment applied [2].

Tyrosine kinase inhibitors (TKIs) play an important role in cancer therapy. Sorafenib, a representative of this group, is one of the two TKIs approved by the Food and Drug Administration for the first-line treatment of HCC [3]. Sorafenib is a modern drug with an antiproliferative and anti-angiogenic effect. It is also used to treat patients with renal cell

Key Points

A single administration of paracetamol increases exposure to sorafenib and sorafenib N-oxide in the brain tissue.

Patients receiving paracetamol during sorafenib therapy may experience intensified adverse reactions from sorafenib.

✉ Agnieszka Karbownik
agnieszkakarbownik@o2.pl

1 Department of Clinical Pharmacy and Biopharmacy, Poznan University of Medical Sciences, 14 Św. Marii Magdaleny Str., 61-861 Poznan, Poland

2 Department of Gynecological Oncology, University Hospital of Lord's Transfiguration, 82/84 Szamarzewskiego Str., 60-569 Poznan, Poland

3 Department of Physical Pharmacy and Pharmacokinetics, Poznan University of Medical Sciences, 6 Święcickiego Str., 60-781 Poznan, Poland

carcinoma (RCC) and thyroid cancer. Moreover, its efficacy has been evaluated in clinical trials in patients with breast cancer, salivary gland cancer, melanoma, non-small-cell lung carcinoma, and glioma. Sorafenib blocks cell signal transduction by binding to the intracellular domains of membrane receptors which belong to the group of tyrosine kinases—VEGFR-1, VEGFR-2, VEGFR-3 (vascular endothelial growth factor receptor 1, 2, 3), PDGFR-β (platelet-derived growth factor receptor β), FLT-3 (fms-like tyrosine kinase 3), FGFR1 (fibroblast growth factor receptor 1) and RET (rearranged during transfection). Sorafenib inhibits serine-threonine kinases such as B-Raf, Raf1 and UGT (UDP-glucuronosyltransferase) isoforms (UGT1A1, UGT1A9) [4–9].

About 55% of cancer patients and up to 66% of metastatic patients with advanced cancer suffer from pain caused by cancer. Paracetamol (acetaminophen) is an antipyretic and non-opioid analgesic. It is a first-degree drug on the analgesic ladder, recommended by the WHO for the treatment of mild and moderate pain in cancer therapy [1]. Its mechanism of action is multidirectional. It inhibits cyclooxygenase (COX) in the arachidonic acid pathway. The central inhibition of the COX-1 and COX-2 isoforms gives an analgesic effect [10–12]. Ayoub et al. [13] proved that paracetamol reduced the concentration of PGE_2 prostaglandins in the brain. Pickering et al. [14] proved that paracetamol affected the serotonergic system by connecting it with 5-HT3 receptors. Research on animals showed the dependence between the use of a TKI (sunitinib) and concomitantly administered paracetamol; the exposure to the TKI and its plasma C_{max} and area under the plasma concentration-time curve decreased [15].

A third of patients with disseminated cancer have brain metastases. The occurrence of metastatic lesions within the central nervous system is a sign of a poor prognosis in the disease progression [16]. Paracetamol is a P-gp inducer in an indirect mechanism, which results in the expression of P-gp in the brain. Tan et al. [17] conducted experiments on mice and observed that the simultaneous administration of paracetamol and sunitinib increased the concentration of the TKI in male brains, but decreased it in female brains.

Our previous pilot study showed that a single administration of sorafenib and paracetamol increased the plasma exposure to sorafenib and its active metabolite [18]. Therefore, the aim of this study was to determine the effect of paracetamol on the degree of sorafenib penetration through the blood–brain barrier (BBB).

2 Materials and Methods

2.1 Chemicals and Drugs

Sorafenib (CAS number 284461-73-0) and sorafenib N-oxide were purchased from LGC Standards (Łomianki, Poland). Lapatinib (CAS number 231277-92-9), methanol, acetonitrile, ethyl acetate, ammonium acetate, glacial acetic acid, sodium hydroxide, and dimethyl sulfoxide (DMSO) were purchased from Sigma-Aldrich (Poznań, Poland). Water used in the mobile phase was deionized, distilled and filtered through a Millipore system (Direct Q3, Millipore, USA) before use. Sorafenib tosylate (Nexavar®, batch number BXHT61) was purchased from Bayer Polska Sp. z o.o., (Warsaw, Poland). Paracetamol (Pedicetamol, batch number K003) and 0.9% NaCl (9 mg/mL, 100 mL) were purchased from Sequoia sp. z o.o. (Warsaw, Poland) and Baxter sp. z o.o (Warsaw, Poland).

2.2 Experimental Animals, Dosing and Sample Collection

The experimental protocol for this study was reviewed and approved by the Local Ethics Committee. All applicable international, national, and/or institutional guidelines for the care and use of animals were followed. Eighty-four adult male Wistar rats (weight 460–505 g) were used in the study so that the plasma and brain tissue might be collected from 3 animals at each analyzed time point. The experimental animals were kept under 12-h light–dark cycles at 23 ± 2 °C, relative humidity ($55 \pm 10\%$) and were provided with food and water ad libitum. The animals were allowed to acclimatize for a week before starting the experiments. The rats were divided into two equal groups—one receiving paracetamol and sorafenib ($n = 42$, I_{SR+PA}) and the other receiving a vehicle (0.9% NaCl) and sorafenib ($n = 42$, II_{SR}). Paracetamol was given directly into the stomach at a dose of 100 mg/kg [19], 30 min prior to sorafenib administration [20]. For oral administration, sorafenib (100 mg/kg b.w. [21]) was dissolved in 1 mL of 10% DMSO. The blood and brain samples were collected at the following time points—0, 0.5, 1, 1.5, 2, 3, 4, 5, 6, 7, 8, 10, 12, and 24 h after administration. Blood (100 μL) was collected from each rat by cutting off a piece of the tail. At sampling times, the animals were killed and their brains were rapidly removed. The blood samples were transferred into heparinized tubes and centrifuged at 2,880*g* for 10 min at 4 °C. The collected brains of the animals were immediately dissected, washed in 0.9% NaCl, divided along the longitudinal axis and homogenized with 0.9% NaCl (4 mL per 1 g of brain) in an Ultra-Turrax homogenizer (Witko, Łódź, Poland).

2.3 HPLC–UV Assays

The concentrations of sorafenib and sorafenib N-oxide were assayed using a high-performance liquid chromatography (HPLC) method with ultraviolet (UV) detection (HPLC Waters 2695 Separations Module with autosampler, Waters 2487 Dual λ Absorbance Detector) [22]. This HPLC method

was adapted to the conditions of our laboratory and fully validated in accordance with the published EMA guideline. Stock solutions of sorafenib and sorafenib N-oxide were prepared by dissolving the drugs in DMSO at a concentration of 1 mg/mL and stored in glass tubes at − 80 °C. Serial (working) dilutions in acetonitrile were prepared from this stock solution for the preparation of calibration and quality control (QC) samples. The internal standard (IS) master stock and working stock were prepared at concentrations of 1 mg/mL and 100 µg/mL in DMSO and acetonitrile, respectively. Both the master and working IS stocks were stored at − 80 °C. Fifty µL of acetonitrile containing IS was added to each plasma sample (20 µL) and vortex-mixed for 20 s. Then, 300 µL of acetonitrile was added to precipitate proteins. Subsequently, all samples were centrifuged at 7,833*g* for 10 min. The supernatant was transferred into glass centrifuge tubes and 1.0 mL Millipore water was added. After vortex-mixing for 2 min, the mixture was successively extracted twice, each with 3.0 mL ethyl acetate (EA). After every addition of EA, the centrifuge tubes were shaken for 25 min at room temperature and then centrifuged for 10 min at 4,867*g*. The EA layer was transferred into a 5-mL flask and the EA layers collected from both extractions were evaporated to dryness under a stream of concentrator at 40 °C. The residue was reconstituted in 80 µL phase (ammonium acetate:acetonitrile = 3:7). Brain homogenate samples were prepared in the same way. Chromatographic separation was carried out on a reversed phase C18 column (Symmetry®C 8, 5 µm 4.6 mm × 250 mm HPLC column). Eluent A consisted of ammonium acetate 0.1 M pH 3.4 (adjusted with glacial acetic acid) and eluent B acetonitrile. Linear gradient started at 60% eluent A and 40% eluent B to 29% eluent A and 71% eluent B. The temperature of the column was maintained at 25 °C. The detection wavelength was set at 265 nm and the injection volume was 20 µL. The column was equilibrated for at least 20 min with the mobile phase at a flow rate of 1 mL/min. The plasma samples were analyzed against the calibration curve, obtained from calibration standards prepared in blank rat plasma. The lower limit of quantification (LLOQ) for sorafenib was 0.1 µg/mL. Intra- and inter-day precision and accuracy of the low QC (0.3 µg/mL), medium QC (1.5 µg/mL), and high QC (3.0 µg/mL) were well within the acceptable limit of 10.5% coefficient of variation (CV%). The calibration curve for sorafenib was linear and ranged from 0.1 to 3.5 µg/mL ($r = 0.997$). The LLOQ for sorafenib N-oxide was 0.02 µg/mL. Intra- and inter-day precision and accuracy of the low QC (0.06 µg/mL), medium QC (0.12 µg/mL), and high QC (0.2 µg/mL) were within the acceptable limit of 12% CV%. The calibration curve for sorafenib N-oxide was linear in the range 0.02–0.25 µg/mL ($r = 0.997$). The brain homogenate samples were analyzed against the calibration curve obtained from calibration standards prepared in ultrapurified water. The LLOQ for sorafenib and sorafenib N-oxide was 0.01 µg/mL. Intra- and inter-day precision and accuracy of the low QC (0.03 and 0.02 µg/mL), medium QC (0.2 and 0.025 µg/mL) and high QC (0.3 and 0.03 µg/mL) were within the acceptable limit of a 14% CV% for sorafenib and sorafenib N-oxide, respectively. The linearity of the method was proved for the range of 0.01–0.4 µg/mL ($r = 0.999$) and 0.01–0.04 µg/mL ($r = 0.998$) for sorafenib and sorafenib N-oxide, respectively. The retention times for lapatinib, sorafenib N-oxide, and sorafenib were 9.0, 12.8, and 15.6 min, respectively. The relative recoveries for sorafenib, sorafenib N-oxide, and lapatinib were 92, 87, 52%, respectively.

2.4 Calculation of Drug Concentration in the Brain

The total concentrations of sorafenib and its metabolite in the rat brain were calculated knowing that 1 µg/mL determined in the brain homogenate resulted in 5 µg/mL in the brain itself, due to the homogenization of 1 g of the tissue with 4 volumes of the 0.9% NaCl solution. The calculated brain concentrations were then corrected for the drug amount in the residual brain blood (Eq. 1), according to the procedure reported by Fridén et al. [23]:

$$C_{b,corr} = \frac{C_b - \left[f_{u,p} \times V_w \times C_p + \left(1 - f_{u,p}\right) \times V_{protein} \times C_p\right] - C_{RBC} \times V_{RBC}}{1 - V_w - V_{RBC}} \quad (1)$$

where $C_{b,corr}$ = the total drug concentration in the brain corrected for the residual blood; C_b = total concentration determined in the brain; C_p = total drug concentration in plasma; C_{RBC} = total drug concentration in red blood cells; $f_{u,p}$ = unbound drug fraction in plasma; V_w, $V_{protein}$, and V_{RBC} = apparent brain vascular spaces of plasma water (10.3 µL/g), plasma proteins (8.0 µL/g), and red blood cells (2.1 µL/g), respectively. As sorafenib is strongly bound to human and rat plasma proteins (about 99.5% [24]), the value of $f_{u,p} = 0$ was used in the calculations for both the parent drug and its N-oxide. The values of C_{RBC} were estimated using Eq. 2 reported in [23]:

$$C_{RBC} = \frac{C_{blood} - C_p \times (1 - Hct)}{Hct} \quad (2)$$

where C_{blood} denoted the total drug concentration in whole blood and Hct was the hematocrit of rat blood (0.45). The C_{blood} values were calculated as 0.893 C_p, based on the rat plasma-to-whole blood sorafenib concentration ratio of 1.12 [24].

2.5 Pharmacokinetic Analysis

Based on the total concentrations of sorafenib and its metabolite in the rat plasma and brain, the area under the curve from zero to 24 h (AUC) was computed in Phoenix

WinNonlin 8.1 (Certara USA Inc., Princeton, USA) using a noncompartmental analysis with a sparse sampling approach. The analysis also provided the standard error (SE) of the AUC estimates, which enabled calculation of the SE for the brain-to-plasma AUC ratio:

$$SE_{\frac{AUC_{brain}}{AUC_{plasma}}} = \frac{1}{AUC_{plasma}} \times SE_{AUC_{brain}} + \frac{AUC_{brain}}{AUC^2_{plasma}} \times SE_{AUC_{plasma}}.$$

The brain-to-plasma partition coefficient (K_p) was calculated as AUC_{brain}/AUC_{plasma}. The tissue uptake efficiency and selectivity were assessed with the K_p and drug targeting index (DTI), which was calculated as a ratio of the K_p in the I_{SR+PA} group to the K_p in the II_{SR} group [25].

3 Results

Changes of the mean concentration of sorafenib and sorafenib N-oxide over time in the plasma and brain are presented in Figs. 1 and 2, respectively. The concentration of sorafenib in the brain samples collected at 0.5 h after drug administration in the II_{SR} group was undetectable. The concentration of sorafenib N-oxide in all the brain samples collected at 0.5, 1, 1.5, 2, and 3 h in the II_{SR} group was also undetectable. Moreover, in the I_{SR+PA} group at 0.5, 1, 1.5 and 2 h, the sorafenib N-oxide levels in the brain samples were below the LLOQ.

The pharmacokinetic profiles of sorafenib and sorafenib N-oxide in the blood plasma and brain were shown to be different between the groups. The pharmacokinetic parameters of the compounds in plasma and brain are listed in Table 1. Paracetamol increased the sorafenib and sorafenib N-oxide plasma AUC in the I_{SR+PA} compared with the II_{SR} group (54.1 vs 32.1 and 3.74 vs 3.05 μg × h/mL, respectively). The C_{max} of sorafenib and sorafenib N-oxide was also higher in the I_{SR+PA} group (2.41 vs 2.13, and 0.19 vs 0.16 μg/mL). The comparison of both groups of animals revealed an increase in the C_{max} and AUC_{0-t} of sorafenib and sorafenib N-oxide in the brain. The brain C_{max} and AUC of the parent drug in the I_{SR+PA} group compared with the II_{SR} group were greater by 49.5 and 77.8%, respectively, and the same parameters for the metabolite were higher by 51.4 and 50.9% (Table 1). The K_p values showed that the effectiveness of sorafenib and sorafenib N-oxide uptake in the brain was the same in both groups (Table 1). The DTI values of sorafenib and sorafenib N-oxide were 1.051 and 1.229.

4 Discussion

The incidence of metastases in patients with HCC is increasing. There may be intra-hepatic and extra-hepatic metastases, with an incidence ranging from 15 to 50%, depending on the cancer stage [26, 27]. The incidence of brain metastases in HCC patients is relatively low (1–6%). The prognosis for these patients is poor and the survival period is several weeks if therapy is not applied. Therefore, brain metastases are considered a terminal state in patients with HCC [28]. The incidence of brain metastases in patients with RCC is approximately 4–7%. There is a poor prognosis for RCC patients with brain metastases, as the median overall survival is only 11 months after diagnosis [29]. Therefore, it is important that targeted therapy applied to patients with brain metastases should be characterized by a high level of tumor penetration, which is usually limited by the activity

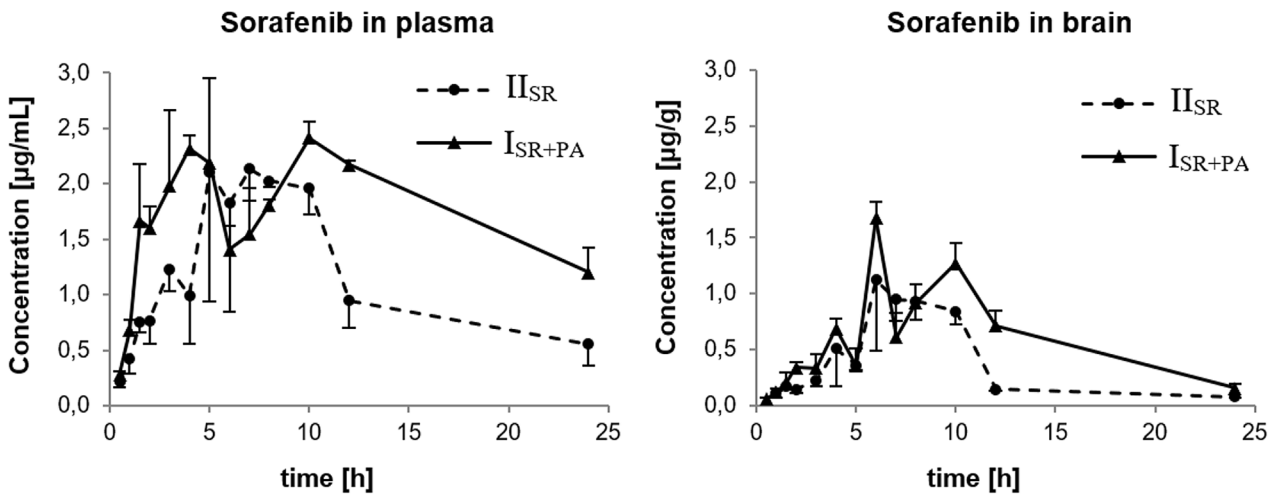

Fig. 1 Plasma and brain pharmacokinetic profiles of sorafenib after oral administration of 100 mg/kg sorafenib dose alone (II_{SR}) or coadministered with 100 mg/kg oral dose of paracetamol (I_{SR+PA}) to rats. Data represent mean ± SD ($n = 3$ per time point)

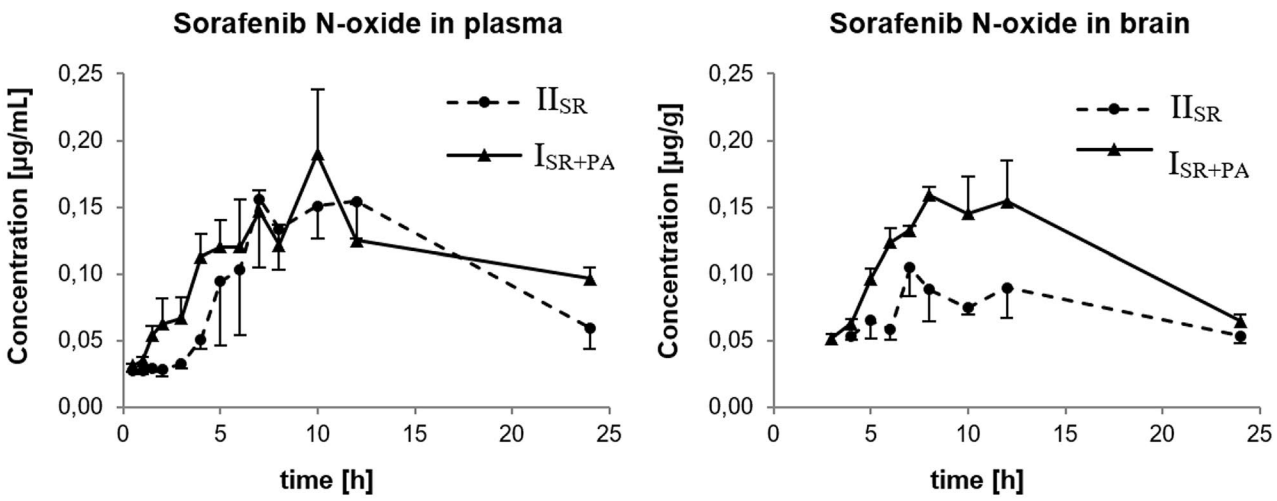

Fig. 2 Plasma and brain pharmacokinetic profiles of sorafenib N-oxide after oral administration of 100 mg/kg sorafenib dose alone (II_{SR}) or coadministered with 100 mg/kg oral dose of paracetamol (I_{SR+PA}) to rats. Data represent mean ± SD ($n = 3$ per time point)

Table 1 Non-compartmental plasma and brain pharmacokinetic parameters of sorafenib and sorafenib N-oxide after oral administration of 100 mg/kg of sorafenib alone (II_{SR}) or coadministered with 100 mg/kg of oral paracetamol (I_{SR+PA})

Pharmacokinetic parameters	I_{SR+PA}	II_{SR}
Blood plasma		
Sorafenib		
C_{max} (µg/mL)[a]	2.41 ± 0.14	2.13 ± 0.28
t_{max} (h)	10.0	7.0
AUC_{0-t} (µg × h/mL)[b]	54.1 ± 1.7	32.1 ± 2.0
Sorafenib N-oxide		
C_{max} (µg/mL)[a]	0.19 ± 0.05	0.16 ± 0.05
t_{max} (h)	10.0	7.0
AUC_{0-t} (µg × h/mL)[b]	3.74 ± 0.14	3.05 ± 0.17
Brain tissue		
Sorafenib		
C_{max} (µg/mL)[a]	1.68 ± 0.14	1.12 ± 0.63
t_{max} (h)	6.0	6.0
AUC_{0-t} (µg × h/mL)[b]	15.6 ± 0.7	8.75 ± 0.48
K_p^b	0.287 ± 0.022	0.273 ± 0.032
Sorafenib N-oxide		
C_{max} (µg/mL)[a]	0.16 ± 0.01	0.10 ± 0.02
t_{max} (h)	8.0	7.0
AUC_{0-t} (µg × h/mL)[b]	3.22 ± 0.13	2.14 ± 0.10
K_p^b	0.862 ± 0.068	0.701 ± 0.073

C_{max} maximum concentration, t_{max} time to reach C_{max}, AUC_{0-t} area under the plasma or brain concentration–time curve from zero to the time of the last measurable concentration (24 h), K_p tissue-to-plasma partition coefficient

[a]Data represent mean ± SD ($n = 3$)

[b]Data represent estimate ± SE for 8–13 points profiles with $n = 3$ animals per each point

of transporters located in the BBB. Research has shown that sorafenib may increase the susceptibility of glioma cells to TTFields [30].

Wolchok et al. reported a patient with metastatic melanoma who was treated with paracetamol administered at a dose of 15 g/m^2 and 80 mg/m^2 carmustine (BCNU). The therapy significantly reduced liver metastases. Response was stabilized and continued throughout the therapy. There was a partial response observed in another patient after two cycles of 20 g/m^2 paracetamol and 10 mg/m^2 BCNU. Both responses were noted at lower than standard BCNU doses. The authors concluded that the improvement in the therapy was either caused by paracetamol alone or paracetamol potentiated the antitumor effect of BCNU [31]. However, this hypothesis has not been confirmed on a larger group of patients. Wu et al. [32] proved that paracetamol increased the cytotoxic activity of cisplatin/paclitaxel in human ovarian cancer in vitro and in in vivo cisplatin treatment. The authors suggested that the inclusion of high doses of paracetamol, which is a widely available drug, into cisplatin- or paclitaxel-based regimens may increase the efficacy of cytostatics in ovarian cancer. Gai et al. [33] noted that when paracetamol was combined with erastin, it induced ferroptosis in non-small-cell lung carcinoma cells, which may be another option of treatment of this cancer. Sorafenib was also found to be one of the few TKIs inhibiting ferroptosis [34].

Paracetamol penetrates through the BBB where it may induce ABCB1 and ABCB2 [17]. On the other hand, Novak et al. [35] observed that paracetamol exhibited a short inhibitory effect on P-gp activity in the intestines, manifested by the increased bioavailability of digoxin (P-gp substrate).

The authors emphasized that the potential occurrence of drug–drug interaction should be taken into consideration when P-gp substrates are co-administered with paracetamol.

Manov et al. [36] found that the activity of P-glycoprotein in cancer cells could be modulated by paracetamol. This finding is very important for cancer patients, who often receive high doses of paracetamol, which may influence the effect of cancer therapy.

Chee et al. [37] found that the administration of ketoconazole resulted in a higher concentrations of sunitinib in the liver, kidney and brain tissues. The C_{max} of sunitinib in the brain doubled after the administration of ketoconazole, whereas the $AUC_{0–inf}$ was 20% higher than in the control group. However, the authors emphasised that the increase in the exposure was not caused by the effect of ketoconazole on the BBB, because the $AUC_{0–inf}$ ratio between the brain tissue and plasma was 2.25 in the control group, whereas in the group under study it decreased to 1.70. This means that the drug penetration across the BBB was in fact less effective in the studied group.

Paracetamol penetrates through the BBB and can modulate the activity of OATP1B1, OATP1B3 and OAT3. It also affects other efflux transporters in the BBB, especially ABCG2 and ABCB1 [20]. When mice were administered paracetamol and sunitinib [20], the exposure to sunitinib decreased by half in male and female animals. Moreover, in the female group the uptake efficiency decreased by 50%, whereas the C_{max} decreased in female and male mice by 32 and 36%, respectively. The constitutive androstane receptor (CAR) is a ligand-activated transcription factor involved in P-gp regulation in the brain microvasculature. Paracetamol is a CAR activator. Our study showed that a single dose of paracetamol increased the levels of sorafenib and sorafenib N-oxide in the plasma and brain. However, the K_p and DTI parameters showed that the uptake efficiency in both groups was comparable. The increase in the plasma drug exposure may have been caused by the influence of paracetamol on intestinal P-gp, which resulted in increased exposure to sorafenib in the brain. Patients receiving paracetamol during sorafenib therapy may experience intensified adverse reactions from sorafenib, especially encephalopathy, peripheral sensory neuropathy, dysgeusia, and depression.

The limitations of our study have to be noted. The sampling protocol was destructive (one-animal-per-sample design). With the use of 84 animals in total, we could provide three individuals per each time point. However, the use of 84 animals was justified by realization of the principle of the 3Rs (replacement, reduction, and refinement). On the other hand, the concentration–time profiles obtained for sorafenib and its N-oxide contained as many as 8–13 points, which supports their robustness. Another limitation of the study was the age of the rats (adult rats), i.e., associated with their high body mass. This in fact facilitated the oral administration of the drug and the collection of blood. Future studies in younger rats are warranted to verify the influence of age on the brain penetration of sorafenib and its N-oxide.

5 Conclusion

It is important to increase the penetration of the drug into the cancer-lesioned tissue in patients with brain metastases. A single administration of paracetamol increases exposure to sorafenib and sorafenib N-oxide in the brain tissue. This effect is likely caused by increased exposure to the parent drug and its metabolite compounds in plasma. The issue warrants further research on larger groups of animals, preferably younger than in our study.

Declarations

Funding The study was financed with an academic grant from the Poznań University of Medical Sciences (Grant no. 502-01-33114230-03592). The funding source had no effect on any part of the study, preparation or submission of the manuscript.

Institutional Ethics Committee Approval All applicable international, national, and/or institutional guidelines concerning the care and use of animals were followed. The experimental protocol for this study was reviewed and approved by the Local Ethics Committee for Animal Experimentation in Poznan (No. 27/2018).

Conflict of Interest All authors declare that they have no conflict of interest.

References

1. WHO guidelines for the pharmacological and radiotherapeutic management of cancer pain in adults and adolescents. January 2019. https://www.who.int/ncds/management/palliative-care/cancer-pain-guidelines/en/. Accessed 7 Aug 2020.
2. Brar G, McNeel T, McGlynn K, Graubard B, Floudas CS, Morelli MP, Xie C, Greten TF, Altekruse S. Hepatocellular carcinoma (HCC) survival by etiology: a SEER-Medicare database analysis. J Clin Oncol. 2019;37:201. https://doi.org/10.1200/JCO.2019.37.4_suppl.201.

3. Target Oncology. Expert discusses sequencing TKI strategies in hepatocellular carcinoma. August 2019. https://www.targetedonc.com/view/expert-discusses-sequencing-tki-strategies-in-hepatocellular-carcinoma. Accessed 7 Aug 2020.
4. Cheng AL, Kang YK, Chen Z, Tsao CJ, Qin S, Kim JS, Luo R, Feng J, Ye S, Yang TS, Xu J, Sun Y, Liang H, Liu J, Wang J, Tak WY, Pan H, Burock K, Zou J, Voliotis D, Guan Z. Efficacy and safety of sorafenib in patients in the Asia-Pacific region with advanced hepatocellular carcinoma: a phase III randomised, double-blind, placebo-controlled trial. Lancet Oncol. 2009;10:25–34. https://doi.org/10.1016/S1470-2045(08)70285-7.
5. Marmé F, Gomez-Roca C, Graudenz K, Huang F, Lettieri J, Peña C, Trnkova ZJ, Eucker J. Phase 1, open-label, dose-escalation study of sorafenib in combination with eribulin in patients with advanced, metastatic, or refractory solid tumors. Cancer Chemother Pharmacol. 2018;81:727–37. https://doi.org/10.1007/s00280-018-3540-9.
6. Evans DM, Fang J, Silvers T, Delosh R, Laudeman J, Ogle C, Reinhart R, Selby M, Bowles L, Connelly J, Harris E, Krushkal J, Rubinstein L, Doroshow JH, Teicher BA. Exposure time versus cytotoxicity for anticancer agents. Cancer Chemother Pharmacol. 2019;84:359–71. https://doi.org/10.1007/s00280-019-03863-w.
7. Tlemsani C, Huillard O, Arrondeau J, Boudou-Rouquette P, Cessot A, Blanchet B, Thomas-Schoemann A, Coriat R, Durand JP, Giroux J, Alexandre J, Goldwasser F. Effect of glucuronidation on transport and tissue accumulation of tyrosine kinase inhibitors: consequences for the clinical management of sorafenib and regorafenib. Expert Opin Drug Metab Toxicol. 2015;11:785–94. https://doi.org/10.1517/17425255.2015.1030392.
8. Qosa H, Avaritt BR, Hartman NR, Volpe DA. In vitro UGT1A1 inhibition by tyrosine kinase inhibitors and association with drug-induced hyperbilirubinemia. Cancer Chemother Pharmacol. 2018;82:795–802. https://doi.org/10.1007/s00280-018-3665-x.
9. Miners JO, Chau N, Rowland A, Burns K, McKinnon RA, Mackenzie PI, Tucker GT, Knights KM, Kichenadasse G. Inhibition of human UDP-glucuronosyltransferase enzymes by lapatinib, pazopanib, regorafenib and sorafenib: implications for hyperbilirubinemia. Biochem Pharmacol. 2017;129:85–95. https://doi.org/10.1016/j.bcp.2017.01.002.
10. Klotz U. Paracetamol (acetaminophen) – a popular and widely used nonopioid analgesic. Arzneimittelforschung. 2012;62:355–9. https://doi.org/10.1055/s-0032-1321785.
11. Graham GG, Scott KF. Mechanism of action of paracetamol. Am J Ther. 2005;12:46–55.
12. Ward B, Alexander-Williams JM. Paracetamol revisited: a review of the pharmacokinetics and pharmacodynamics. Acute Pain. 1999;2:139–49. https://doi.org/10.1016/S1366-0071(99)80006-0.
13. Ayoub SS, Colville-Nash PR, Willoughby DA, Botting RM. The involvement of a cyclooxygenase 1 gene-derived protein in the antinociceptive action of paracetamol in mice. Eur J Pharmacol. 2003;538:57–65.
14. Pickering G, Loriot MA, Libert F, Eschalier A, Beaune P, Dubray C. Analgesic effect of acetaminophen in humans: first evidence of a central serotonergic mechanism. Clin Pharmacol Ther. 2006;79:371–8.
15. Slosky LM, Thompson BJ, Sanchez-Covarrubias L, Zhang Y, Laracuente ML, Vanderah TW, Ronaldson PT, Davis TP. Acetaminophen modulates P-glycoprotein functional expression at the blood-brain barrier by a constitutive androstane receptor-dependent mechanism. Mol Pharmacol. 2013;84:774–86. https://doi.org/10.1124/mol.113.086298.
16. Posner JB. Management of brain metastases. Rev Neurol (Paris). 1992;148:477–87.
17. Tan SY, Wong MM, Tiew AL, Choo YW, Lim SH, Ooi IH, Modamio P, Fernández C, Mariño EL, Segarra I. Sunitinib DDI with paracetamol, diclofenac, mefenamic acid and ibuprofen shows sex-divergent effects on the tissue uptake and distribution pattern of sunitinib in mice. Cancer Chemother Pharmacol. 2016;78:709–18. https://doi.org/10.1007/s00280-016-3120-9.
18. Karbownik A, Sobańska K, Grabowski T, Stanisławiak-Rudowicz J, Wolc A, Grześkowiak E, Szałek E. In vivo assessment of the drug interaction between sorafenib and paracetamol in rats. Cancer Chemother Pharmacol. 2020;85:1039–48. https://doi.org/10.1007/s00280-020-04075-3.
19. Gandia P, Saivin S, Lavit M, Houin G. Influence of simulated weightlessness on the pharmacokinetics of acetaminophen administered by the oral route: a study in the rat. Fundam Clin Pharmacol. 2004;18(1):57–64.
20. Liew MH, Ng S, Chew CC, Koo TW, Chee YL, Chee EL, Modamio P, Fernández C, Mariño EL, Segarra I. Sunitinib-paracetamol sex-divergent pharmacokinetics and tissue distribution drug–drug interaction in mice. Investig New Drugs. 2017;35:145–57. https://doi.org/10.1007/s10637-016-0415-y.
21. Wang X, Zhang X, Liu F, Wang M, Qin S. The effects of triptolide on the pharmacokinetics of sorafenib in rats and its potential mechanism. Pharm Biol. 2017;55:1863–7. https://doi.org/10.1080/13880209.2017.1340963.
22. Afify S, Rapp UR, Högger P. Validation of a liquid chromatography assay for the quantification of the Raf kinase inhibitor BAY 43-9006 in small volumes of mouse serum. J Chromatogr B Anal Technol Biomed Life Sci. 2004;809:99–103.
23. Fridén M, Ljungqvist H, Middleton B, Bredberg U, Hammarlund-Udenaes M. Improved measurement of drug exposure in the brain using drug-specific correction for residual blood. J Cereb Blood Flow Metab. 2010;30:150–61. https://doi.org/10.1038/jcbfm.2009.200.
24. Nexavar. INN-Sorafenib – European Medicines Agency. Scientific discussion. https://www.ema.europa.eu/en/documents/scientific-discussion/nexavar-epar-scientific-discussion_en.pdf. Accessed 4 Feb 2020.
25. Oberoi RK, Mittapalli RK, Elmquist WF. Pharmacokinetic assessment of efflux transport in sunitinib distribution to the brain. J Pharmacol Exp Ther. 2013;347:755–64. https://doi.org/10.1124/jpet.113.208959.
26. Fukuoka K, Masachika E, Honda M, Tsukamoto Y, Nakano T. Isolated metastases of hepatocellular carcinoma in the left atrium, unresponsive to treatment with sorafenib. Mol Clin Oncol. 2015;3:397–9.
27. Jo S, Shim HK. A patient who has survived for a long period with repeated radiotherapies for multifocal extrahepatic metastases from hepatocellular carcinoma. Radiat Oncol J. 2013;31:267–72. https://doi.org/10.3857/roj.2013.31.4.267.
28. Kamimura K, Kobayashi Y, Takahashi Y, Abe H, Kumaki D, Yokoo T, Kamimura H, Sakai N, Sakamaki A, Abe S, Takamura M, Kawai H, Yamagiwa S, Terai S. Tumor markers for early diagnosis for brain metastasis of hepatocellular carcinoma: a case series and literature review for effective loco-regional treatment. Cancer Biol Ther. 2017;18:79–84. https://doi.org/10.1080/15384047.2016.1276134.
29. Hu D, Hu Y, Li J, Wang X. Symptomatic treatment of brain metastases in renal cell carcinoma with sorafenib. J Cancer Res Ther. 2018;14(Supplement):S1223–6. https://doi.org/10.4103/0973-1482.189402.
30. Jo Y, Kim EH, Sai S, Kim JS, Cho JM, Kim H, Baek JH, Kim JY, Hwang SG, Yoon M. Functional biological activity of sorafenib as a tumor-treating field sensitizer for glioblastoma therapy. Int J Mol Sci. 2018;19:E3684. https://doi.org/10.3390/ijms19113684.
31. Wolchok JD, Williams L, Pinto JT, Fleisher M, Krown SE, Hwu WJ, Livingston PO, Chang C, Chapman PB. Phase I trial of high dose paracetamol and carmustine in patients with metastatic melanoma. Melanoma Res. 2003;13:189–96.

32. Wu YJ, Neuwelt AJ, Muldoon LL, Neuwelt EA. Acetaminophen enhances cisplatin- and paclitaxel-mediated cytotoxicity to SKOV3 human ovarian carcinoma. Anticancer Res. 2013;33:2391–400.
33. Gai C, Yu M, Li Z, Wang Y, Ding D, Zheng J, Lv S, Zhang W, Li W. Acetaminophen sensitizing erastin-induced ferroptosis via modulation of Nrf2/heme oxygenase-1 signaling pathway in non-small-cell lung cancer. J Cell Physiol. 2020;235:3329–39. https://doi.org/10.1002/jcp.29221.
34. Sun X, Niu X, Chen R, He W, Chen D, Kang R, Tang D. Metallothionein-1G facilitates sorafenib resistance through inhibition of ferroptosis. Hepatology. 2016;64:488–500. https://doi.org/10.1002/hep.28574.
35. Novak A, Carpini GD, Ruiz ML, Luquita MG, Rubio MC, Mottino AD, Ghanem CI. Acetaminophen inhibits intestinal p-glycoprotein transport activity. J Pharm Sci. 2013;102:3830–7. https://doi.org/10.1002/jps.23673.
36. Manov I, Bashenko Y, Hirsh M, Iancu TC. Involvement of the multidrug resistance P-glycoprotein in acetaminophen-induced toxicity in hepatoma-derived HepG2 and Hep3B cells. Basic Clin Pharmacol Toxicol. 2006;99:213–24.
37. Chee EL, Lim AY, Modamio P, Fernandez-Lastra C, Segarra I. Sunitinib tissue distribution changes after coadministration with ketoconazole in mice. Eur J Drug Metab Pharmacokinet. 2016;41:309–19. https://doi.org/10.1007/s13318-015-0264-7.